ACS APPLIED MATERIALS & INTERFACES

Research Article

www.acsami.org

Novel Nitrocellulose Membrane Substrate for Efficient Analysis of Circulating Tumor Cells Coupled with Surface-Enhanced Raman Scattering Imaging

Peng Zhang, Ren Zhang, Mingxia Gao,* and Xiangmin Zhang*

Department of Chemistry and Institute of Biomedical Sciences, Fudan University, Shanghai 200433, China

Supporting Information

ABSTRACT: The capture and detection of circulating tumor cells (CTCs) in the bloodstream of patients with cancer is crucial for the clinical diagnosis and therapy. In the present work, a facile and integrated approach based on novel nitrocellulose membrane substrate and large-scale surface-enhanced Raman scattering (SERS) imaging technology has been developed for CTCs' sensitive detection and enumeration. The system mainly consists of three aspects: capture of CTCs in bloodstream, SERS probes labeling of the captured CTCs and large-scale SERS imaging readout of CTCs enumeration. The NC membrane was used to prepare the novel CTC-capture substrate through antibody self-assembled. It was low-cost, easily prepared and completely nontoxic. Furthermore, excellent capture efficiency of the substrate was demonstrated using nonsmall-cell lung cancer (NSCLC) cells (NCI-H1650) as target cells. As the most sensitive detection technology, SERS holds huge potential in CTCs analysis. Large-scale SERS imaging was employed in CTCs enumeration for the first time, instead of the conventional fluorescence imaging. Our SERS probes, with a simplified structure, offered highly enough sensitivity to recognize every single cell clearly. In the simulation experiment of spiking 100 cancer cells into 1 mL of human whole blood, 34 cells were captured and counted successfully according to the SERS imaging result. Our experimental results demonstrate the potential feasibility of novel NC membrane substrate coupled with large-scale SERS imaging technology for the accurate enumeration of CTCs in human whole blood.

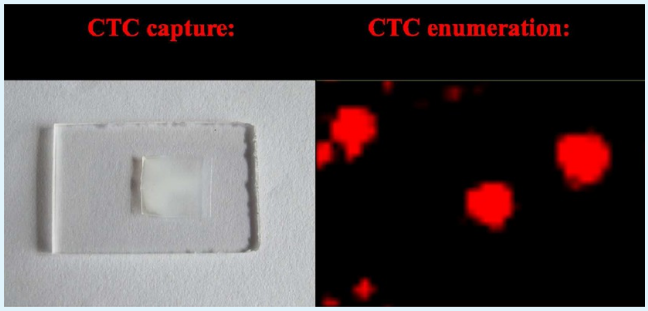

KEYWORDS: *circulating tumor cells, nitrocellulose membrane substrate, large-scale surface-enhanced Raman scattering imaging*

INTRODUCTION

Circulating tumor cells (CTCs) are shed from cancerous tumors, enter the circulatory system, and migrate to distant organs to form metastases that ultimately lead to the death of most patients with cancer.[1] Therefore, the detection of CTCs could provide a novel approach to screening, detection of recurrence and evaluation of treatment response for kinds of cancers. CTCs are rare, in only up to hundreds of cells mL^{-1}, whereas comprising 10^9 common hematologic cells per milliliter in the peripheral blood of patients with metastatic cancer.[2−4] Hence, detecting rare CTCs is a tremendous technical challenge, mainly consisting of two aspects, how to capture CTCs efficiently from the complex hematological background and how to recognize the signal of single CTCs accurately and sensitively.

Over the past decade, several strategies involving immunomagnetic beads,[5,6] ISET (isolation by size of epithelial tumor cells),[7] and microfluidic devices[8−14] have been proposed to isolate CTCs. Although these methods represent important advances in this field, much improvement is still needed. The only FDA-approved CTC enumeration method is cell-search assay, which uses antibody coated magnetic beads for CTC isolation and has been applied for clinical treatment widely, whereas it suffers from low CTC-capture efficiency. ISET is based on cell size difference, thus a potential concern with this method is the impurity of leukocytes, leading to a high false-positive rate. Microfluidic devices, modified with capture ligands including antibodies and aptamers, are considered to hold vast potential in dealing with microliter amounts of blood sample. However, most efforts for increasing the CTC-capture efficiency were based on engineering complicated structures inside the microfluidic devices, such as microposts, sinusoidal channels and silicon nanopillars. These structures make the devices fabrication time-consuming, meanwhile cost too much unavoidably, which are not compatible for the widely used and high-throughput blood sample analysis. In the very recent years, paper-based microbiosensers represented a new and outstanding approach for the advantages of extremely low cost and ease of fabrication. Chromatography paper[15] and filter paper[16] have been used to construct SERS substrate assays by

Received: October 7, 2013
Accepted: December 9, 2013
Published: December 9, 2013

modifying the surface chemistry and patterning nanoparticles. Nitrocellulose membranes (NCs),[17] with the natural capability of protein adsorption and outstanding biocompatibility, could be an ideal CTC−capture substrate.

Highly sensitive fluorescence imaging technology, using organic dyes or Quantum dots (QDs) fluorescence probes, has been widely used in cell imaging and biomedical diagnostics.[18,19] However, the fluorescence analysis has its inherent disadvantages: broad emission band spectra, strong background autofluorescence interference and photobleaching of fluorescence probes. Furthermore, fluorescence-based imaging techniques often lack the sensitivity and selectivity to environmental conditions of biological samples. Recently, SERS technology holds vast potential as a highly sensitive and selective tool for the identification of biological analytes, thus has attracted a great deal of interest. The electromagnetic field enhancement arising from localized surface plasmon resonance (LSPR) around the metallic surface can magnify the Raman signal intensity by as much as 10−14 orders of magnitude, which even been sufficient for single molecule detection.[20] SERS gives a sharp fingerprint-like spectral pattern, which is distinct from other interferences within the complex biological milieu. In contrast, fluorescence spectra could be disguised by strong scattering signals from cells and protein clusters at low signal intensities, such as rare CTC events. In addition, SERS retains stable in water or other biocompatible environment, capable for multiplex detection in single detection systems, and even the fingerprints can indicate rich molecular and structural information. In the most recent, several reports have attempted to detect CTCs in human whole blood employing SERS technology.[6,21−25] The experimental results indicated SERS technology hold greater potential in CTCs detection, thus we have an intense desire to employ large-scale SERS imaging for CTCs enumeration and replace the conventional fluorescence imaging completely.

In this study, we integrated a novel CTC-capture substrate and facile SERS probes for SERS imaging analysis of CTCs in human peripheral blood. The CTC-capture substrate was prepared based on the NC membrane and PMMA wafer. After transparency treatment and antibody conjunction, this novel cell-capture substrate has been demonstrated to be cost efficient, robust, easily prepared, compatible for the follow-up SERS imaging detection, and more importantly have high cell capture efficiency. The SERS probes were fabricated directly using a bifunctional molecule p-mercaptobenzoic acid (pMBA), a widely used Raman reporter molecule, binding with antibodies through the condensation reaction of carboxyl-amine.[26] It provided so intense SERS signal that the single cell can be distinguished accurately. This integrated platform was employed to detect CTCs in the blood, satisfied results were achieved. According to the SERS imaging detection, as low as 20 cells in PBS buffer can be counted accurately and some dozens of cells were also detected efficiently in the 100 cancer cells spiked whole bloods.

EXPERIMENTAL SECTION

Reagents and Materials. Hydrogen tetrachloroaurate ($HAuCl_4 \cdot 3H_2O$), sodium citrate, *p*-mercaptobenzoic acid (pMBA), 1-ethyl-3-[3-dimethy-laminopropyl] carbodiimide hydrochloride (EDC), *N*-hydroxysuccinimide (NHS), bovine serum albumin (BSA), and some other chemical reagents were purchased from Sigma-Aldrich Inc. (St. Louis, MO, U.S.A.). Antibody mouse anti-human EpCAM-CD326 was ordered from Biolegend (U.S.A.). The cancer cell lines nonsmall-cell lung cancer (NSCLC) NCI-H1650, liver cancer cell 7703 were acquired from Shanghai cell bank, Chinese academy of sciences. RPMI 1640 media, fetal bovine serum and penicillin-streptomycin were purchased from HyClone (U.S.A.). Nitrocellulose membranes were obtained from Kenker (U.S.A.). PMMA wafer was offered by YuTong (Shanghai, China). All buffers were prepared in deionized water and then passed through a membrane filter with a 0.22 μm pore size.

Preparation of the CTC-Capture Substrate. The commercially purchased NC membrane was cut into small pieces (1 cm ×1 cm). Subsequently, the NC membrane piece was immerged in pure ethanol for 10 s for the transparency process and then tiled on the PMMA wafer. After they were washed and activated with PBS buffer, 20 μL antibodies (0.5 μg/μL) in 80 μL PBS buffer were dropped onto the NC membrane and reacted in 37 °C for 0.5 h. Antibodies were adsorbed on the surface of NC membrane tightly and the adsorption capacity can be analyzed by high performance capillary electrophoresis (HPCE). At last, 1% BSA solution was employed to block the nonspecific adsorption sites. After washing three times with PBS buffer, the prepared NC membrane substrate was stored in 4 °C for further use.

Synthesis of the SERS Probes. The colloid Au nanoparticles (60 nm) were prepared according to the classical Frens' method.[27] In a typical process, 100 mL of 0.01% $HAuCl_4$ aqueous solution was heated to boiling with vigorous stirring, and then 0.75 mL of 1% trisodium citrate solution was added. The mixture was kept boiling for 0.5 h. Afterward, the solution was allowed to cool down to room temperature with continuous stirring.

The prepared Au nanoparticles were washed with 2 mM borate buffer for three times by centrifuging the solution with 3000 rpm for 0.5 h, and resuspended in borate buffer. A total of 5 μL of 1 mM Raman reporter molecules (pMBA) in ethanol was added to 1.0 mL of Au nanoparticles, and the resultant mixture was allowed to gently shake for 2 h, the reporter-labeled nanoparticles were then separated from the solution by centrifugation at 3000 rpm for 0.5 h and retained in 1.0 mL PBS buffer (10 mM). Afterward, 100 μL of 0.5 mg/mL monoclonal antibody mouse antihuman EpCAM CD326, 2 mg of EDC, and 2 mg of NHS were added to 1.0 mL of pMBA-labeled Au nanoparticles with gentle agitation separately. After incubation at 37 °C for 2 h, the pMBA-labeled immunogold nanoparticles were purified by centrifugation and resuspended with 1.0 mL of PBS buffer. Then 10 μL of BSA (5%) was added to the above pMBA-labeled immunogold nanoparticles to make sure that no bare sites on Au nanoparticles were left. The mixture was incubated for 1 h at 37 °C and then stored in 4 °C refrigerator after washing three times.

Cell Culture and SERS Probes Labeling. In this work, non-small-cell lung cancer cells (NCI-H1650) was used as the target cell, EpCAM-negative liver cancer cell line 7703 as a negative control. These two types of cells were cultured in RPMI 1640 media, under a humidified atmosphere (5% CO_2 plus 95% air) at 37 °C. Medias were supplemented with 10% fetal bovine serum and 1% penicillin-streptomycin.

The cells were harvested with 0.25% Trypsin−EDTA when maturated and resuspended in PBS buffer with the ideal concentration about 100 cells per microliter. Appropriate amount of cells were loaded onto the cell-capture substrate. After incubating at 37 °C for 1 h, the substrate was gently washed with PBS at least 3 times. The captured cells were then reacted with SERS probes for another 0.5 h. We washed with PBS 3 times to remove the excess SERS probes. The target cells on the substrate were fixed with 4% paraformaldehyde and subsequently detected by SERS measurement.

Raman Measurements. The Raman measurements were performed with a Renishaw Invia Raman microscope system. A Spectra Physics argon-ion laser operating at 633 nm was used as the excitation source with a laser power of 3 mW. The Rayleigh line was removed from the collected Raman scattering using a holographic notch filter in the collection path. All SERS spectra reported here were the results of a single 10 s accumulation. A charge-coupled device (CCD) camera was coupled to a spectrograph that in combination provided a 2 cm^{-1} spectral resolution. Raman images were obtained

using a Raman point-mapping method. It created a spectral image by measuring the Raman spectrum of each pixel of the image, one at a time. A computer-controlled $x-y$ translation stage was used in a 1 μm step size.

RESULTS AND DISCUSSION

We integrated a novel NC membrane substrate for highly efficient capture of CTCs and facile SERS probes for SERS imaging analysis of CTCs in human peripheral blood. As illustrated in scheme 1, the whole experimental process consisted of functionalization of NC membrane substrate, selective isolation of CTCs, fabrication of SERS probes, SERS probes labeling and sensitive SERS imaging detection. The ultimate goal of the system is to capture and count the CTCs in the bloodstream of cancer patients accurately.

Scheme 1. Schematic Illustration of CTCs Capture and SERS Imaging Detection

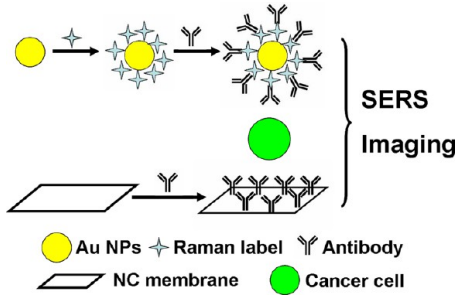

Enriching rare CTCs from human whole blood is the key challenge for eliminating complex background interference and improving the detection sensitivity. The NC membrane was employed to prepare the CTC-capture substrate through antibody self-assembled. It was nontoxic and widely used in protein immobilization and immunoassays, hence can attach antibodies for specific binding with CTCs naturally. After the transparency treatment in pure ethanol and immobilization on the PMMA wafer, the NC membrane coated PMMA substrate was robust, transparent and flat enough for the following SERS imaging detection, seen in Figure 1D. NSCLC NCI-H1650 cells have high level expression of EpCAM, with at least 500000 antigens per cell,[8] resulting in stable antibody–antigen interaction. We employed FITC-conjugated EpCAM to test the selectivity of antibodies. According to flow cytometry results (refer to Figure S1 in the Supporting Information), excellent bonding efficiency was demonstrated and unspecific interaction was minimum. The amount of immobilized antibodies on the NC membranes was measured by HPCE. Compared the signal peak areas before and after adsorption (shown in Supporting Information Figure S2), the density of antibodies on the substrate was up to 10 $\mu g/cm^2$, which offered a powerful guarantee of the high capture efficiency.

The absorption specificity of the cell-capture substrate was confirmed using NCI-H1650 cells as target cells. The cell concentration was adjusted to 100 cells/μL in PBS buffer, and 10 μL of cell suspensions was spotted onto the NC membrane substrate and kept in 37 °C incubator for 1 h. After rinsed with PBS buffer three times, the captured cells were counted by bright field microscope (Nikon). As a control, the NC membrane substrate without antibody immobilization was also examined in parallel. As shown in Figure 1A and 1B, the antibody-functionalized substrate can capture most of the cells, while there was no cell adsorption on the substrate without antibody attachment. To compare these two kinds of substrates in a spatially close experimental setting, we immobilized antibodies only on the left side of the substrate. In Figure 1C, the left side of the substrate captured lots of cells, conversely the right side nearly no cell. This is consistent with the results obtained individually under the separate experimental conditions. The NC membrane had high affinity to membrane proteins of cells indeed, meanwhile the nonspecific absorption was proved to be minimum after BSA blocking. For comparison, EpCAM-negative cancer cell line liver cancer 7703

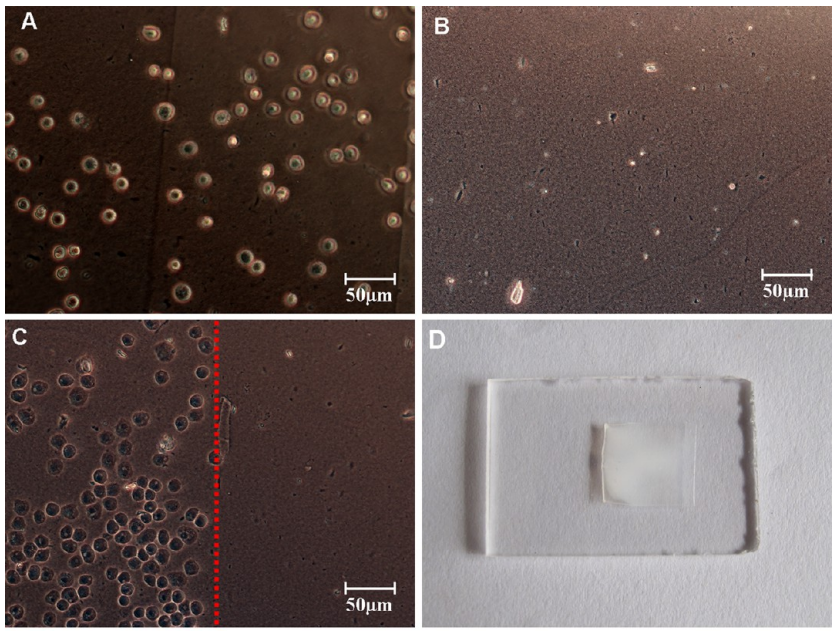

Figure 1. Bright field microscopy images of A. Captured cells in antibody absorbed NC substrate B. Blank control without antibody attachment C. Direct comparison of cell-capture substrate with/without antibody D. Photo of prepared cell-capture substrate.

was also employed to test the capture performance. Relatively low cell numbers were observed and the highly capture specificity of the NC membrane substrate was demonstrated eventually.

Generally, the capture efficiency of the cell capture substrate fell significantly with the target cell number decrease, thus we have measured the capture yield in various amounts of cells ranging from 10000 to 20. The results were shown in Table 1.

Table 1. Cell Capture Efficiency of NC Membrane Substrate for Cancer Cells in PBS Buffer

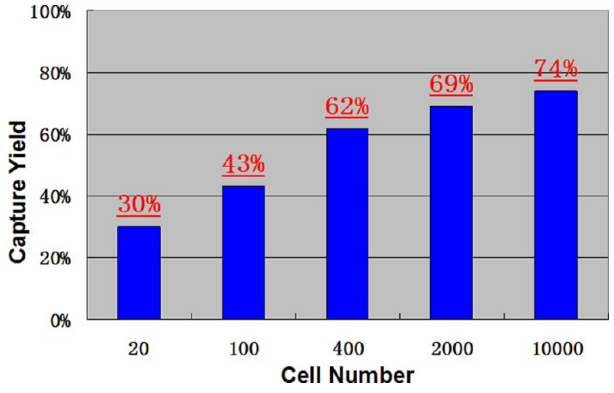

When cells were more than 400, the calculated capture efficiency was above 60%, which was comparable with the previous reports.[8] Even only 20 cells were spiked into PBS buffer, 6 cells were still captured successfully. These results not only confirmed the outstanding cell capture performance, but also showed the potential capability of capturing even several CTCs in whole blood.

In modern SERS analysis, SERS probes always consist of the metallic nanoparticles, the Raman reporter molecules and the specialized attach agents such as antibodies and aptamers.[28−31] The design and fabrication of the SERS probe is generally considered one of the most critical aspects. Unlike the previous reports,[22,32] we utilized 60 nm gold nanoparticles as cores, *p*-mercaptobenzoic acid (pMBA) as both Raman reporter and antibody conjugation agent, resulting in a much simplified structure. Scheme 1 illustrates the complete fabrication process of SRES probes. Gold colloid nanoparticles have already been used in rheumatism treatment for hundreds of years for the perfect biocompatibility and nontoxicity.[33] Moreover, Gold nanoparticles have advantages including long-term stability, easily controllable size distribution, high homogeneity and high LSPR enhancement, which make it very suitable for SERS analysis. According to the previous study,[22] 60 nm gold nanoparticles, showing higher SERS enhanced efficiency than others with smaller diameter, hence were chose to prepare the SERS probes in this experiment.

On the basis of the classic Frens' one-step method, stable and homogeneous gold nanoparticles were synthesized simply. The TEM image was listed in Figure 2A and the estimated average diameter was 60 nm. These gold nanoparticles were then functionalized with pMBA to introduce carboxyl groups for conjugating with antibodies and act as Raman reporter molecule at the same time. pMBA has been widely used in SERS probes due to its strong affinity to the surfaces of gold nanoparticles through Au−S bond, strong SERS signals and multifunctionalized character of carboxyl groups.[34] The carboxyl groups of pMBA molecules can form stable amide bonds with the antibody molecules under the participation of EDC and NHS. The HPCE results (Supporting Information Figure S2) revealed that about sixty percent of antibodies were conjugated to SERS probes, corresponding to 30 μg antibodies per milliliter SERS probes solution. The white layers (about 5 nm) on the surface of gold nanoparticles in TEM image (Figure 2B) also confirmed the successful conjugation of antibodies. In the previous mainstream reports, the gold nanoparticles were covered with a mixture of two different thiolates, referred to as multilayer SERS probes. One thiolate bound with antibodies covalently and the other acted as Raman reporter molecule. This multilayer probes can tune the SERS signals easily with spectrally distinct Raman reporter molecules, greatly facilitating multiplexed applications. Contrarily, the so-called monolayer probes use the bifunctional molecule pMBA to replace the two kinds of thiolates. This fabrication protocol is a much more facile route, simplified and straightforward, which is very important for improving the stability and reproducibility of SERS probes. Furthermore, we no longer need to adjust the

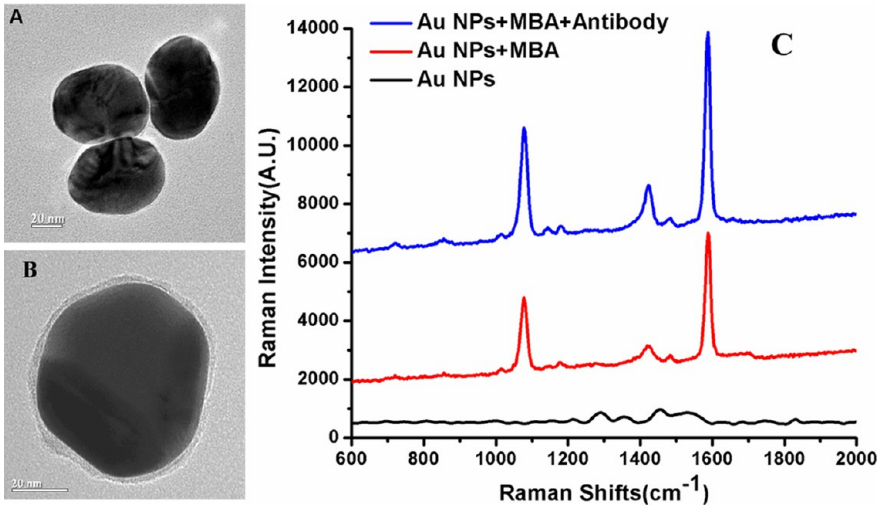

Figure 2. (A) TEM image of synthesized 60 nm gold nanoparticles (B) The TEM image of antibody conjugated SERS probe (C) The SERS spectra of pure gold nanoparticles, pMBA functionalized gold nanoparticles and antibodies conjugated gold nanoparticles.

dx.doi.org/10.1021/am404406c | ACS Appl. Mater. Interfaces 2014, 6, 370−376

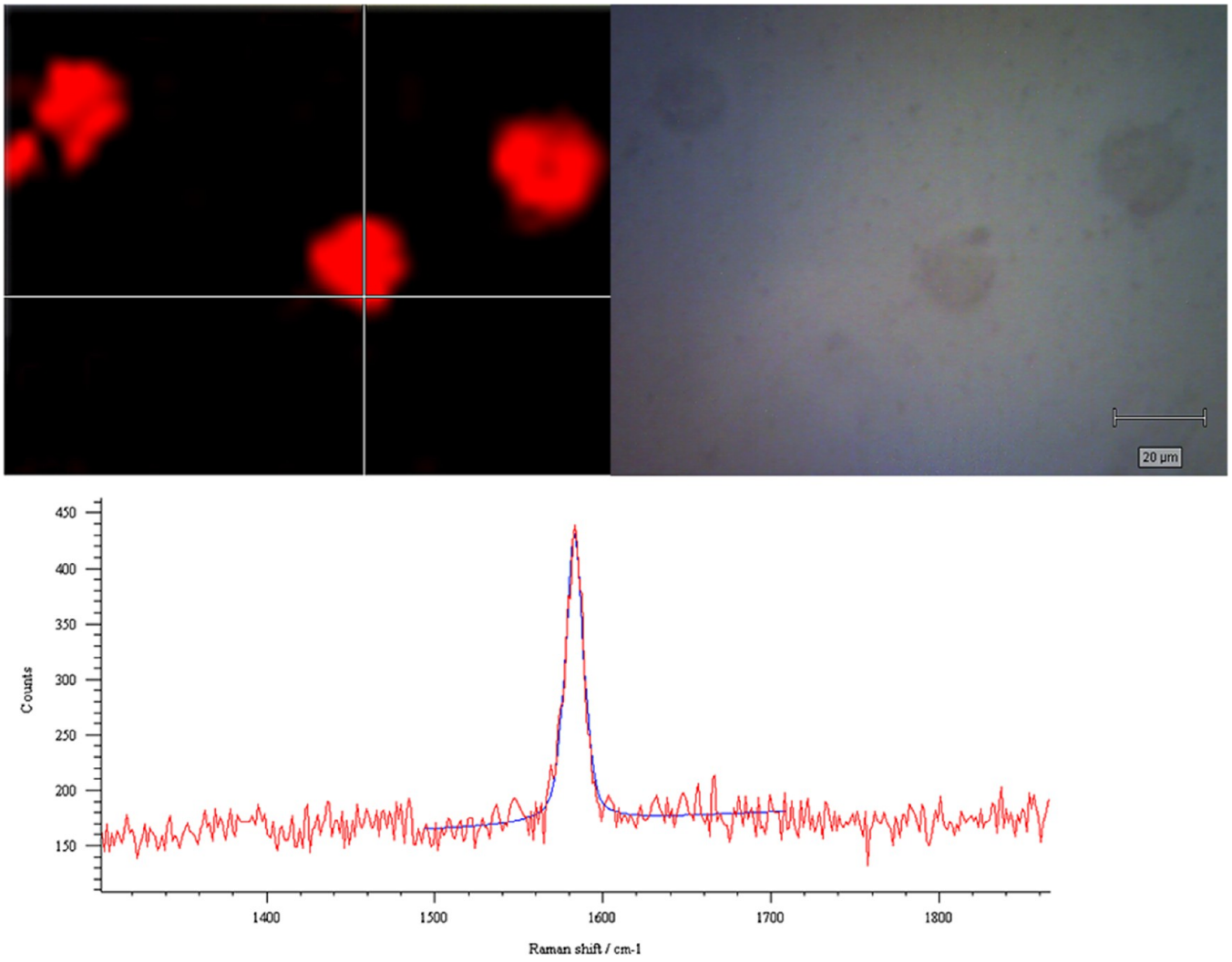

Figure 3. Overlay image of Raman mapping and bright field for target cells.

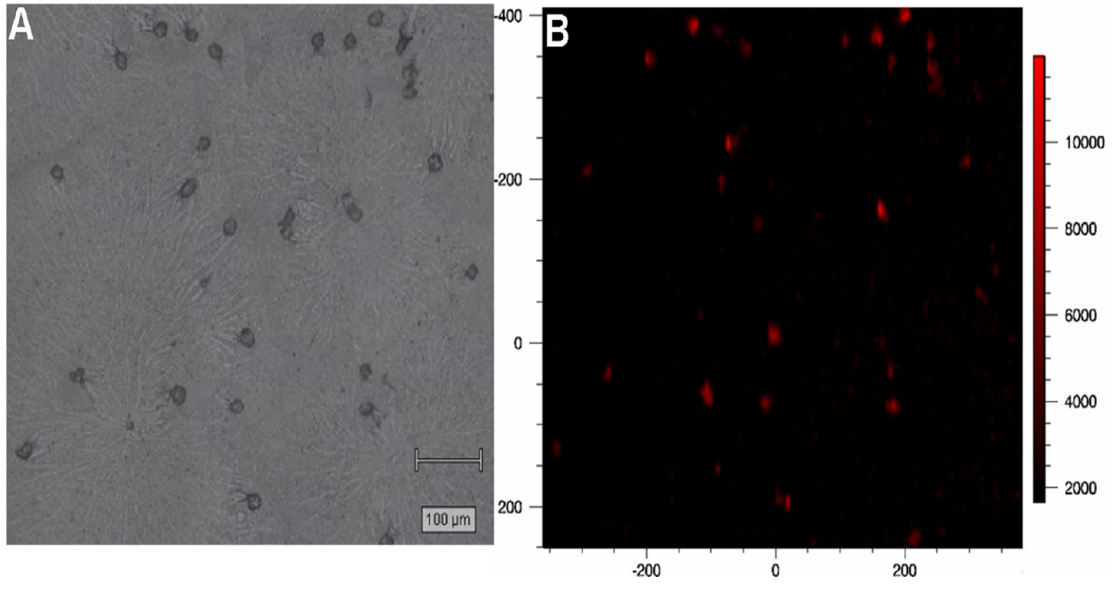

Figure 4. Large-scale SERS image of NCI-H1650 cells and corresponding bright field image.

ratio of Raman reporter and antibodies conjugation molecules. All the surface of gold nanoparticles was covered by pMBA, which can also enhance the Raman signal and antibodies conjugation.

dx.doi.org/10.1021/am404406c | ACS Appl. Mater. Interfaces 2014, 6, 370−376

Figure 2C shows the SERS spectra of pure gold nanoparticles, pMBA functionalized gold nanoparticles before and after antibodies attachment, respectively. The characteristic Raman peaks of SERS probes were 1077 and 1586 cm^{-1}, corresponding to the ring breathing and axial deformation of pMBA. Considering the protonated effect of EDC and break of the citrate protective layer, the antibody conjugation process may lead to a slight aggregation to form more "hot spots". Nonetheless, the "hot spots" provided by the light aggregation can increase the Raman signals greatly. This also explained why the antibody conjugated SERS probes had much stronger Raman signal than those before antibody attachment.

The captured cells were labeled with SERS probes through the specific antibody−antigen interaction. Supporting Information (refer to Figure S3A and 3B) firmly confirmed the specificity of our SERS probes. Summarily speaking, each of the target cells NCI-H1650 was labeled with SERS probes successfully and intense SERS characteristic signal was detected, while the liver cancer cells 7703 had negative SERS signal in the control experiment. In addition, the NC membrane substrate also showed minimal unspecific adsorption of SERS probes, providing a clear background for SERS cell imaging. The high specificity of SERS probes was crucial for distinguishing target cancer cells from the other complex components in whole blood such as leukocytes and lymphocytes. Figure 3 shows the SERS and bright field images of NCI-H1650, respectively. The clear SERS mapping image was fitted and observed based on the strong characteristic SERS peak at 1586 cm^{-1}. From the parallel two pictures, the cells images were corresponded one by one strictly; even the detailed cell shape and surface outline were nearly the same. Furthermore, the same color of cell SERS images indicated the uniform attachment of SERS probes on the surface of target cells. The intense SERS signal of single cell, the clear background and the minimal unspecific attachment indicated that the SERS imaging technology can serve as the readout of single cancer cell recognition. The large-scale SERS imaging of captured NCI-H1650 cells in NC membrane substrate was shown in Figure 4. The bright field and SERS images of NCI-H1650 cancer cells in Figure 4A and 4B also corresponded to each other perfectively, indicating that our SERS imaging technology holds the capability to distinguish and enumerate every single cancer cell accurately. SERS imaging technology shows huge potential to replace the conventional fluorescence imaging in CTC counting.

To simulate the detection and enumeration of CTCs in patient whole blood, 100 NCI-H1650 cells were spiked into 1 mL healthy donators' whole blood. After erythrocyte lyses with Tris-NH_4Cl buffer and 1000 rpm low-speed centrifugation, the cancer cells were separated with the serum preliminarily. The nucleated cells mixture was spotted on the NC membrane substrate, the target cells were specifically captured and the other leukocytes and lymphocytes washed away. The Raman imaging was processed following the SERS labeling, as it can not only count the cancer cells, but also verify the captured target cells once again. Part of the SERS imaging photo was shown in Figure 5, in which each red dot means a CTC. According to the SERS imaging result, 34 cancer cells were detected and counted eventually. Compared with previously reported work,[8] the ultimate detection efficiency of our integrated approach was slightly lower. The main reason lies on the low surface-volume ratio of the NC membrane, resulting in the less physical contact between the cells and NC membrane and the loss of cells in the washing process. Integration of NC membrane substrate and microfluidic chips should be an ideal improvement in further study, which could increase fluidic agitation and minimize the washing loss simultaneously. However, this is a new attempt to recognize and enumerate cancer cells using NC membrane substrate and SERS imaging, also predicting the huge potential in future clinical applications.

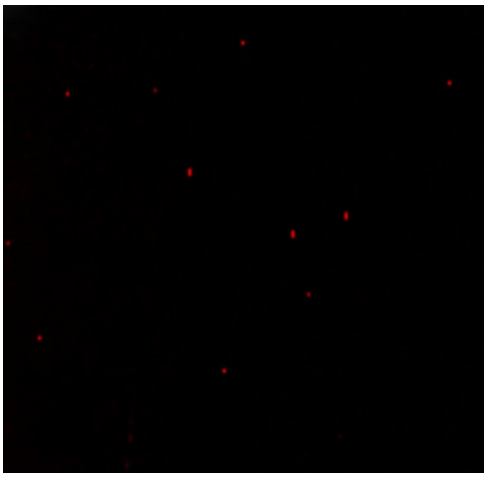

Figure 5. SERS image of spiked cancer cells in human whole blood.

CONCLUSION

We employed a novel NC membrane substrate as platform for the analysis of CTCs in human whole blood coupled with SERS imaging technology successfully. The CTC-capture substrate based on the Nitrocellulose membrane was low-cost, easily prepared and even used as cell-capture substrate for the first time. Nevertheless, satisfied capture results was achieved, which was comparable with other much more complex devices. The SERS probes conjugated with antibodies and Raman reporters can recognize the target cancer cells specifically. Especially the uses of bifunctional molecule pMBA, not only simplify the fabrication process, but also contribute more intense Raman signal, which was very important for the perfect SERS imaging results. According to the SERS imaging pictures, every single cell can be distinguished accurately, even the detailed shape and outline was very clear. The successful enumeration of cancer cells in simulated patient whole bloods shows the further clinical application future of our approach.

ASSOCIATED CONTENT

Supporting Information

Detailed experimental process and additional results. This information is available free of charge via the Internet at http://pubs.acs.org/.

AUTHOR INFORMATION

Corresponding Authors

*Tel.:+86 21 65643983. Fax: +86 21 65641740. E-mail: mxgao@fudan.edu.cn.

*Tel.:+86 21 65643983. Fax: +86 21 65641740. E-mail: xmzhang@fudan.edu.cn.

Notes

The authors declare no competing financial interest.

■ ACKNOWLEDGMENTS

This work was supported by National Basic Research Program of China (Project 2012CB910604), the National High-Tech R&D Program (Project 2012AA020202), and the National Natural Science Foundation of China (Project: 21275034 and 21175026).

■ REFERENCES

(1) Mehlen, P.; Puisieux, A. *Nat. Rev.Cancer* **2006**, *6*, 449−458.
(2) Pantel, K.; Alix-Panabieres, C. *Trends. Mol. Med.* **2010**, *16*, 398−406.
(3) den Toonder, J. *Lab Chip* **2011**, *11*, 375−377.
(4) Pantel, K.; Brakenhoff, R. H.; Brandt, B. *Nat. Rev. Cancer* **2008**, *8*, 329−340.
(5) Cristofanilli, M.; Budd, G. T.; Ellis, M. J.; Stopeck, A.; Matera, J.; Miller, M. C.; Reuben, J. M.; Doyle, G. V.; Allard, W. J.; Terstappen, L.; Hayes, D. F. *N. Engl. J. Med.* **2004**, *351*, 781−791.
(6) Sha, M. Y.; Xu, H. X.; Natan, M. J.; Cromer, R. *J. Am. Chem. Soc.* **2008**, *130*, 17214−17217.
(7) Vona, G.; Sabile, A.; Louha, M.; Sitruk, V.; Romana, S.; Schutze, K.; Capron, F.; Franco, D.; Pazzagli, M.; Vekemans, M.; Lacour, B.; Brechot, C.; Paterlini-Brechot, P. *Am. J. Pathol.* **2000**, *156*, 57−63.
(8) Nagrath, S.; Sequist, L. V.; Maheswaran, S.; Bell, D. W.; Irimia, D.; Ulkus, L.; Smith, M. R.; Kwak, E. L.; Digumarthy, S.; Muzikansky, A.; Ryan, P.; Balis, U. J.; Tompkins, R. G.; Haber, D. A.; Toner, M. *Nature* **2007**, *450*, 1235−1239.
(9) Wang, S. T.; Wang, H.; Jiao, J.; Chen, K. J.; Owens, G. E.; Kamei, K. I.; Sun, J.; Sherman, D. J.; Behrenbruch, C. P.; Wu, H.; Tseng, H. R. *Angew. Chem., Int. Ed.* **2009**, *48*, 8970−8973.
(10) Hosokawa, M.; Hayata, T.; Fukuda, Y.; Arakaki, A.; Yoshino, T.; Tanaka, T.; Matsunaga, T. *Anal. Chem.* **2010**, *82*, 6629−6635.
(11) Dharmasiri, U.; Njoroge, S. K.; Witek, M. A.; Adebiyi, M. G.; Kamande, J. W.; Hupert, M. L.; Barany, F.; Soper, S. A. *Anal. Chem.* **2011**, *83*, 2301−2309.
(12) Stott, S. L.; Hsu, C. H.; Tsukrov, D. I.; Yu, M.; Miyamoto, D. T.; Waltman, B. A.; Rothenberg, S. M.; Shah, A. M.; Smas, M. E.; Korir, G. K.; Floyd, F. P.; Gilman, A. J.; Lord, J. B.; Winokur, D.; Springer, S.; Irimia, D.; Nagrath, S.; Sequist, L. V.; Lee, R. J.; Isselbacher, K. J.; Maheswaran, S.; Haber, D. A.; Toner, M. *Proc. Natl. Acad. Sci. U. S. A.* **2010**, *107*, 18392−18397.
(13) Arya, S. K.; Lim, B.; Rahman, A. R. A. *Lab Chip* **2013**, *13*, 1995−2027.
(14) Wang, Y. Y.; Zhou, F.; Liu, X. L.; Yuan, L.; Li, D.; Wang, Y. W.; Chen, H. *ACS Appl. Mater. Interfaces* **2013**, *5*, 3816−3823.
(15) Yu, W. W.; White, I. M. *Anal. Chem.* **2010**, *82*, 9626−9630.
(16) Lee, C. H.; Hankus, M. E.; Tian, L.; Pellegrino, P. M.; Singamaneni, S. *Anal. Chem.* **2011**, *83*, 8953−8958.
(17) Bishnoi, S. W.; Lin, Y. J.; Tibudan, M.; Huang, Y. M.; Nakaema, M.; Swarup, V.; Keiderling, T. A. *Anal. Chem.* **2011**, *83*, 4053−4060.
(18) Allard, W. J.; Matera, J.; Miller, M. C.; Repollet, M.; Connelly, M. C.; Rao, C.; Tibbe, A. G. J.; Uhr, J. W.; Terstappen, L. *Clin. Cancer. Res.* **2004**, *10*, 6897−6904.
(19) Hutter, E.; Maysinger, D. *Microsc. Res. Tech.* **2011**, *74*, 592−604.
(20) Zhang, R.; Zhang, Y.; Dong, Z. C.; Jiang, S.; Zhang, C.; Chen, L. G.; Zhang, L.; Liao, Y.; Aizpurua, J.; Luo, Y.; Yang, J. L.; Hou, J. G. *Nature* **2013**, *498*, 82−86.
(21) Qian, X. M.; Peng, X. H.; Ansari, D. O.; Yin-Goen, Q.; Chen, G. Z.; Shin, D. M.; Yang, L.; Young, A. N.; Wang, M. D.; Nie, S. M. *Nat. Biotechnol.* **2008**, *26*, 83−90.
(22) Wang, X.; Qian, X. M.; Beitler, J. J.; Chen, Z. G.; Khuri, F. R.; Lewis, M. M.; Shin, H. J. C.; Nie, S. M.; Shin, D. M. *Cancer Res.* **2011**, *71*, 1526−1532.
(23) Lee, S.; Kim, S.; Choo, J.; Shin, S. Y.; Lee, Y. H.; Choi, H. Y.; Ha, S. H.; Kang, K. H.; Oh, C. H. *Anal. Chem.* **2007**, *79*, 916−922.
(24) Yang, J.; Wang, Z. Y.; Zong, S. F.; Song, C. Y.; Zhang, R. H.; Cui, Y. P. *Anal. Biol. Chem.* **2012**, *402*, 1093−1100.
(25) Huang, J. Y.; Zong, C.; Xu, L. J.; Cui, Y.; Ren, B. *Chem. Commun.* **2011**, *47*, 5738−5740.
(26) Yang, J.; Wang, Z. Y.; Tan, X. B.; Li, J.; Song, C. Y.; Zhang, R. H.; Cui, Y. P. *Nanotechnology* **2010**, *21*, 345101−345109.
(27) Frens, G. *Nat. Phys.* **1973**, *241*, 20−22.
(28) Ni, J.; Lipert, R. J.; Dawson, G. B.; Porter, M. D. *Anal. Chem.* **1999**, *71*, 4903−4908.
(29) Grubisha, D. S.; Lipert, R. J.; Park, H. Y.; Driskell, J.; Porter, M. D. *Anal. Chem.* **2003**, *75*, 5936−5943.
(30) Zhang, D. M.; Ansar, S. M. *Anal. Chem.* **2010**, *82*, 5910−5914.
(31) Carrillo-Carrion, C.; Armenta, S.; Simonet, B. M.; Valcarcel, M.; Lendl, B. *Anal. Chem.* **2011**, *83*, 9391−9398.
(32) Wang, G. F.; Park, H. Y.; Lipert, R. J. *Anal. Chem.* **2009**, *81*, 9643−9650.
(33) De, M.; Ghosh, P. S.; Rotello, V. M. *Adv. Mater.* **2008**, *20*, 4225−4241.
(34) Chen, S.; Yuan, Y.; Yao, J.; Han, S.; Gu, R. *Chem. Commun.* **2011**, *47*, 4225−4227.